Research Article doi: 10.18081/2333-5106/014-04/277-287

Endotoxemia-suppress cardiac function through dysregulation of mitochondrial biogenesis in mice model

Michele M. Bracale, Robyn B. Wonderge, Min Zhou, Evelyn G. Hazen[1*]

Abstract

Sepsis exaggerated proinflammatory response to infection that can progress to carries a significant cardiac dysfunction associated with morbidity and mortality. Mitochondrial biogenesis is involved in the control of cell metabolism, signal transduction, and regulation of mitochondrial reactive oxygen species (ROS) production. We are hypothesis that impairment of biogenesis has been invoked in the pathogenesis of myocardial endotoxemia. C57/BL6 mice were treated with LPS (0.5 mg/kg, iv) for 4 hrs. cardiac function was assessed using a microcatheter. Electronmicroscopy and confocal microscopy revealed that mitochondrial biogenesis is reduced after treatment the mice with LPS compared with control. Further, endotoxemic mice exhibited worse LV function than the control. The exaggerated cardiac contractile depression in LPS treated mice is associated with greater densities of neutrophils and mononuclear cells in the myocardium, and higher levels of TNF-α, IL-1β and IL-6 in the circulation and myocardium. This study will provide insights into mitochondrial biology, the relevance to sepsis, and therapeutic opportunities that possibly emerge.

Keywords: Sepsis, LPS, Proinflammatory response, Cardiac dysfunction, Biogenesis

Introduction

Sepsis is redefined as life-threatening organ dysfunction caused by a dysregulated host response to infection. Severe patients with septic shock require vasopressors to maintain a mean arterial pressure of 65 mmHg in the absence of hypovolemia or present with hyperlactacidemia (serum lactate level > 2 mmol/L) [1].

A higher serum lactate level reflects a systemic metabolic dysfunction induced by an insufficient consumption of nutrients, such as glucose. Mitochondria are the key cellular organelles responsible for nutrient metabolism and energy production [2]. Sepsis-induced mitochondrial damage or dysfunction is the major cause of cellular metabolism disturbance, insufficient energy production, and accompanied oxidative stress, which evoke apoptosis in both organ cells and immune cells and finally lead to immunologic dissonance, multiple organ failure, and

even death in patients [3]. Accordingly, well protection from mitochondrial disorders is critical to reserve cell homeostasis and might be a significant cause of better prognoses [4].

Autophagy is activated after irreversible mitochondrial damage for clearance, while mitochondrial biogenesis is activated through the AMPK/PGC-1a/NRF-1/2 signaling pathway. Insufficient ATP production resulted in ATP/ADP ratio disturbance-activated AMPK and the following PGC-1a/NRF-1/2 pathway, consequently contributing to TFAM expression [5]. TFAM is a promoter of mtDNA expression after its translocation into the mitochondrial matrix and evokes its biogenesis. In both septic patients and animal models, enhanced PGC-1α expression is consistently observed and correlated with a better prognosis [6].

However, AMPK/PGC-1α signaling has a universal effect on cell biology, and its targeting therapeutic strategy might lead to other unbeneficial effects. As a result, much more specific treatment targeted to TFAM is reliable. Currently, recombinant human TFAM (rhTFAM) has been generated and performs well in animal experiments [7].

The impact of rhTFAM has been identified to increase mtDNA expression and improve mitochondrial function in various target organs. Furthermore, it can effectively pass through the blood-brain barrier and protect multiple organs from endotoxin challenge, such as the brain, heart, lung, liver and kidney, accompanied by reduced mortality in septic animals [3].

If sepsis-induced mitochondrial dysfunction is, at least partially, due to a mitochondrial reprogramming, it is legitimate to query the evolutionary advantage of a coordinated activation of pathways leading to a decrease in cell metabolism and energy production. An answer could come from looking at similarities in the heart's response to sepsis and ischemia.

Myocardial hibernation is a well-described phenomenon in the human heart that occurs following ischemia and results in an adaptive downregulation of myocardial oxidative metabolism and function. This protective process sacrifices cardiac contractility to decrease energetic demands and match a reduced oxygen supply, therefore preventing ATP depletion, excessive ROS production and cardiomyocyte death [8]. The metabolic phenotype of the hibernating ischemic heart in human patients and experimental animals matches what is seen in nature in species that undergo seasonal hibernation or similar 'metabolic shut-down' processes such as torpor or estivation [9]. Myocardial hibernation has not been extensively described outside cardiac ischemia and hypoxia, but sepsis is one of the diseases in which hibernation has been proposed to play a role [10]. Changes compatible with cardiac hibernation were seen in the hearts of experimental septic animals, with an increase in myocardial glucose uptake, glucose transporter levels and glycogen storage [11]. Proposed mediators of this metabolic suppression include hormones, inflammatory mediators or endogenous gases such as NO, CO and hydrogen sulfide. These gaseous signalling molecules act in various ways, including inhibition of complex IV and activation of various transcription factors that regulate mitochondrial gene expression (e.g. Nrf2 or hypoxia-inducible factor 1) [12]. Indeed, the administration of exogenous donors of CO or hydrogen sulphide has shown positive effects in experimental sepsis [13]. The coordinated genomic response observed in the septic human

heart further supports a cardiac-specific hibernation, with a decrease in the expression of genes involved not only in ATP production but also ATP consumption (i.e. sarcomeric contraction and excitation-contraction coupling) [14].

We are hypothesis that impairment of biogenesis has been invoked in the pathogenesis of myocardial endotoxemia.

Patients and Methods

Mice were housed under standard conditions of light, temperature, and humidity, with unlimited access to water and food (pelleted rodent food). LPS was injected ip in a single dose of 10 mg/kg body weight. Measurements were performed at different time points (0–24 h) after LPS administration. As control group, animals were handled in parallel and received the same volume of saline solution (vehicle). Animal treatment was carried out in accordance to the [1]Institute of Molecular Medicine, University of Buenos Buenos Aires, Argentina.

Body temperature

Body temperature was determined by measuring rectal temperature in animals using a digital thermometer (MT-Esatherm Ltd. 8172, Czech Republic) with a 2 mm sensor diameter.

NO-hemoglobin (NO-Hb) in blood by electron paramagnetic resonance (EPR)

Micewere anesthetized [ketamine (50 mg/kg) plus xylazine (0.5 mg/kg)], and blood was obtained by cardiac puncture and immediately stored at 77 K (liquid N2) until analyzed. The EPR spectrum of NO-Hb was determined at 77 K in a Bruker spectrometer ECS 106 (Karlsruhe, Germany) with an ER 4102ST cavity. The parameters of the spectra were as follows: field modulation frequency, 50 kHz; microwave frequency, 9.42; modulation amplitude, 4.75 G; microwave power, 10 mW; time constant, 164 ms; sweep width, 800 G; center field, 3300 G [5]. The quantification of the spectra was performed by calculating the area under the curve (double integral of the spectrum). The results are expressed in arbitrary units.

Tissue processing for transmission electron microscopy and micrograph analysis

Mice were anesthetized with [ketamine (50 mg/kg) plus xylazine (0.5 mg/kg)], and hearts were rapidly removed and washed with 0.1 M K2HPO4/KH2PO4, pH 7.4. The left ventricular myocardium was removed and cut into 1 mm3 cubes. Tissue sample was fixed with 2.5% glutaraldehyde in 0.1 M K2HPO4/KH2PO4 (pH 7.4) for 2 h and postfixed in 1% osmium tetroxide in 0.1 M K2HPO4/ KH2PO4 for 1.5 h at 0 1C.

Samples were contrasted with 5% uranyl acetate for 2 h at 0 1C, dehydrated, and embedded in Durcupan resin (Fluka AG, Switzerland) for 72 h at 60 1C. Ultrathin sections were cut and observed with a Zeiss EM 109 transmission electron microscope (Oberkochen, Germany). Representative digital images were captured using a CCD GATAN ES1000W camera (CA, USA). Random sections were selected for analysis by an electron microscopy technician blinded to the treatments. Using the "point counting grids" methodology [15], mitochondrial

density was determined. Damaged mitochondria [16] and mitochondria with swelling were also analyzed. The damaged mitochondrial index included mitochondria with internal vesicles, cristae and membrane disruption, and cleared matrix.

DNA extraction and quantification

DNA was extracted as previously described [17]. Quantification was performed by real-time PCR (StepOne Plus, Life Technologies, Foster City, CA, USA) using two pairs of primers (Table 1) amplifying a single copy region of the genome located on chromosome 3 in the region corresponding to the Topoisomerase I gene (Top1), and a mitochondrial genomic region outside the larger deletion corresponding to the NADH dehydrogenase I gene (mt-Nd1). All amplicons are 153 bp in length. The reaction was carried out in triplicate for each primer pair used, and for each treatment/control. Mitochondrial DNA comparative quantification was analyzed by the algorithm 2-ΔΔCt method [18].

Western blot analysis

Cardiac left ventricle was removed and homogenized in a Bio-Gen pro200 homogenizer (Pro Scientific) in 1 ml of ice-cold Western blot buffer (50 mM Hepes, 100 mM NaCl, 1 mM EDTA, 20 mM NaF, 20 mM Na4P2O7, NaVO3 1 mM, 1% Triton X-100, 1% SDS, pH 7.4; plus 1 mg/ml peptatin, 1 mg/ml aprotinin, 1 mg/ml leupeptin, and 0.4 mM phenylmethanesulfonyl fluoride). After a 10 min incubation at 2 1C, the sample was sonicated twice (30 s with 1 min interval) and centrifuged at 800g for 20 min.

The supernatant was used for Western blot analysis. Equal amounts of proteins (50 μg) were separated by SDS-PAGE (7.5, 10, or 12%) and blotted into nitrocellulose films. Nonspecific binding was blocked by incubation of the membranes with 5% nonfat dry milk in PBS for 1 h at room temperature. Membranes were probed with 1:500 diluted goat polyclonal antibodies against PGC1 [PGC-1 (K-15): sc-5816; Santa Cruz Biotechnology, Santa Cruz, CA], mtTFA [mtTFA (V-13): sc-30965; Santa Cruz Biotechnology, Santa Cruz, CA], LC3B [LC3B antibody (2775); Cell Signaling Technology, MA], p62 [SQSTM1 (P-15): sc-10117; Santa Cruz Biotechnology, Santa Cruz, CA], or mouse monoclonal anti β-actin [β-actin (C4): sc-47778; Santa Cruz Biotechnology, Santa Cruz, CA].

The nitrocellulose membrane was subsequently incubated with a secondary rabbit anti-goat antibody (Santa Cruz Biotechnology, Santa Cruz, CA), rabbit anti-mouse antibody [(315-035-048) Jackson InmunoResearch, Baltimore Pike, USA], or goat anti-rabbit antibody [(GAR):170-5046; Bio-Rad, CA] conjugated with horseradish peroxidase (dilution 1:10,000 or 1:5,000) and revealed by chemiluminescence with ECL reagent. Band images were quantified digitally, using SCION image software, and data were expressed as relative to β-actin expression [17].

Statistical analysis

Results were expressed as mean values7SEM and represent the mean of five independent experiments. ANOVA followed by Dunnett test or Bonferroni test was used to analyze differences among experimental groups. Statistical significance was considered at P<0.05.

Results

Body temperature and NO-Hb levels Six hours after LPS injection, animals showed a significant increase in body temperature with respect to the control group (control: 37.170.2 1C, P<0.05), whereas 12 h after LPS injection, the animals showed significant hypothermia (P<0.01) (Fig. 1). Fig. 1A shows three typical spectra corresponding to blood NO-Hb signals. Fig. 2B shows NO-Hb signal quantification. NO-Hb levels were found increased in endotoxemic animals at every time point analyzed.

Mitochondrial biogenesis time course A 92 kDa protein was identified by Western blot analysis reacting with anti-PGC-1α antibodies in left ventricle homogenate. Its expression was significantly increased at all time points analyzed after LPS injection, as determined by densitometric quantitation of the bands.

Results are shown in Fig. 2A. In addition, levels of mtTFA expression were found significantly increased at 6–24 h of LPS treatment (Fig. 2B). Since cytochrome oxidase is exclusively located in mitochondria (inner membrane), the ratio between its activity in the homogenate and in mitochondrial fractions is a useful tool for analyzing mitochondrial mass [6]. Table 1 shows a significant increase (20%, P<0.05) in this parameter only 24 h after LPS injection. Fig. 3 shows mitochondrial and nuclear DNA quantification.

After 18 h, mitochondrial DNA levels were observed significantly decreased by 67% compared to control and 6 h LPS groups. However, no significant difference was observed at 24 h after LPS treatment with respect to the control group. This observation suggests a recovery in the amount of mitochondrial DNA at 24 h. As a first approach to evaluate the occurrence of autophagy, p62 and LC3 expressions were analyzed.

p62 expression was found significantly increased at 6 h after LPS treatment followed by a time-dependent decrease of the expression (Fig. 3A). LC3-II expression was observed significantly increased at all time points analyzed (Fig. 3B). In order to evaluate morphological changes associated with fusion/fission processes involved in mitochondrial biogenesis, the ultrastructure of left ventricle cardiomyocytes was analyzed by transmission electron microscopy. Control rats displayed normal mitochondrial morphology including well-defined double membranes with normal cristae arrangements and preserved morphology and size.

Six and 18 h after LPS administration, mitochondria displayed several abnormalities, such as formation of internal vesicles (Fig. 4C, H, and I) loss and/or disruption of cristae (Fig. 4D), cleared matrix and swelling (Figs.4, H, and I), and cleared matrix with loss of vacuoles and crests (Fig. 4C).

Twenty-four hours after LPS administration, mitochondria of different sizes and mitochondrial structures compatible with the fission/fusion processes were observed (Figs. 4J and K). However, some cristae disruption and mitochondrial swelling were still observed. Mitochondrial volume density was significantly increased (18%, P<0.001) 6 h after the treatment; at 18 and 24 h the values showed no significant differences with respect to control value (Table 1). The quantification of damaged mitochondria (including swelling, loss and/or disruption of cristae, cleared matrix, and internal vesicles) showed increased values (2 to 1.6 times with respect to control value) 6–24 h after the treatment with LPS (Table 1).
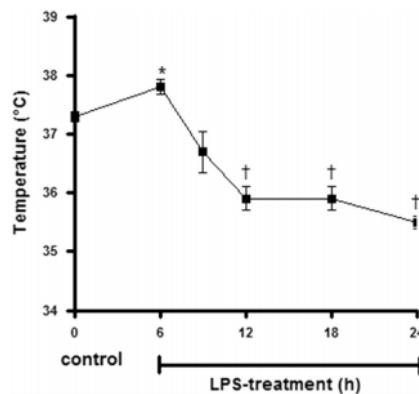

Figure 1.

Body temperature in control and LPS-treated animals. n Po0.05 as compared with control group by ANOVA-Dunnett test. † Po0.01 as compared with the control group, ANOVA-Dunnett test.
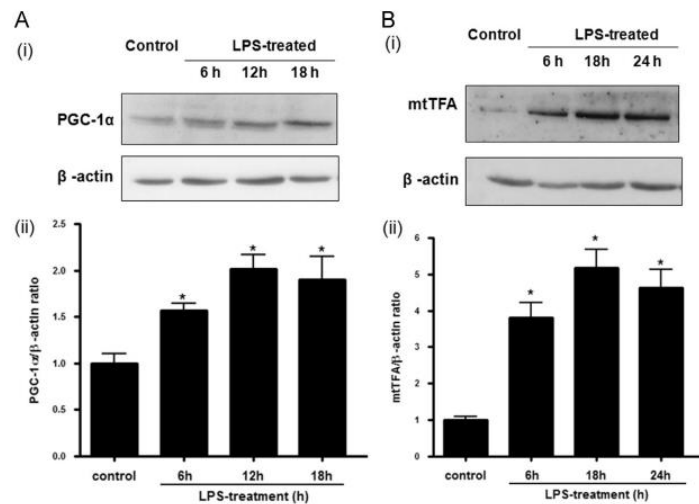

Figure 2.

PGC-1α (A) and mtTFA (B) protein expression of left ventricle myocardium homogenate from control and LPS-treated animals. Panel (i) shows typical examples of Western blots of cardiac homogenates samples. ß-Actin was used as loading control. Bars in panel (ii) figure represent densitometric analysis of PGC-1α/ß-actin ratio or mtTFA/ß-actin ratio blot measurements. n Po0.05 as compared with control group, ANOVA-Dunnett test.
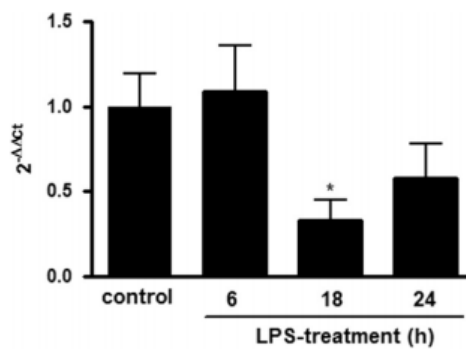
Figure 3.

Cardiac mitochondrial DNA comparative quantification with respect to nuclear DNA measured by real-time PCR and calculated by the quantification algorithm 2-ΔΔCt, for the different time points analyzed. Primers amplifying NADH dehydrogenase 1 gene (mt-Nd1) for mtDNA and Topoisomerase 1 gene (Top1) for nuclear DNA, were used (see Table 1). n Po0.05 as compared with control group, ANOVA Dunnett test.
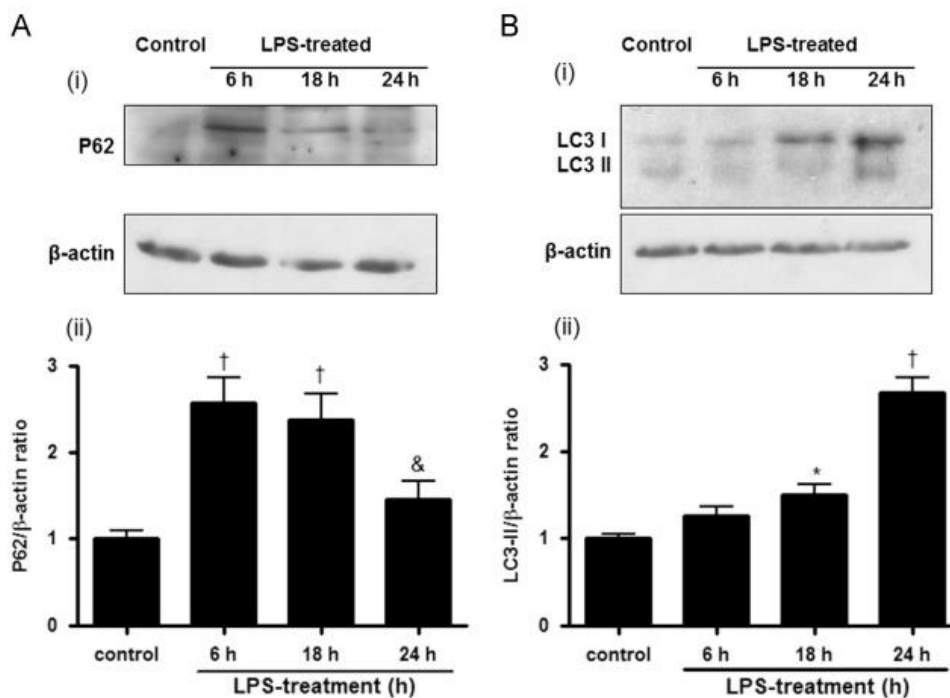

Figure 4.

p62 (A) and LC3 (B) protein expression of left ventricle myocardium homogenate from control and LPS-treated animals. Panel (i) shows typical examples of Western blots of cardiac homogenates samples. ß-Actin was used as loading control. Bars in panel (ii) represent densitometric analysis of p62/ß-actin ratio or LC3-II/ß-actin ratio blot measurements. n Po0.05 as compared with control group, ANOVA-Dunnett test. † Po0.01 as compared with control group, ANOVA-Dunnett test. & Po0.01 as compared with LPS group (6 h), ANOVA-Bonferroni test.

Table 1.

Cardiac cytochrome oxidase activity, as a marker of mitochondrial mass, in control and LPS-treated animals.

	Cytochrome oxidase activity		Activity ratio
	Homogenate k'_1 (min^{-1})/g tissue	Mitochondria k'_2 (min^{-1})/mg protein	Homogenate/mitochondria k'_1/ k'_2 (mg protein/g tissue)
Control	497 ± 8	46.8 ± 1.6	10.7 ± 0.5
LPS 6 h	407 ± 32	41.5 ± 1.5	9.7 ± 0.5
LPS 9 h	604 ± 61	60.1 ± 3.7†	10.0 ± 0.7
LPS 12 h	486 ± 33	50.1 ± 3.4	9.7 ± 0.5
LPS 18 h	526 ± 24	46.1 ± 1.3	11.4 ± 0.5
LPS 24 h	517 ± 31	39.1 ± 1.8*	13.9 ± 1.2*

Discussion

Increased levels of NO, oxidative stress, and elevated AMP/ATP ratio, among others, have been described as signals inducing mitochondrial biogenesis [18]. In this report, blood NO levels, a marker of the occurrence of the inflammatory process, were observed increased at 6 h after LPS treatment and remained increased during all the other time points assessed. This is a very fast and transient increase in NO production; in acute endotoxemia it has been described that the inflammatory response peak is observed between 6 and 10 h after LPS challenge [19].

In line with this observation, we previously described that mitochondrial NO production and functional activity of mtNOS were significantly increased at 6 h after LPS treatment [8]. The accepted view is that the effect of NO on mitochondrial biogenesis is a general phenomenon; NO effects can be differentially analyzed regarding steadystate levels reached and origin. On the one hand, under basal conditions, it was shown that a moderate NO increase, not only produced by eNOS [11] but provided by NO-donors as N-acetylpenicillamine [3], was able to activate mitochondrial biogenesis in rodent muscle cells and adipocytes. Decreased mitochondrial mass, accompanied with a decrease in O2 consumption and ATP levels, was observed, in gastrocnemius muscle of eNOS-deficient animals [20].

In pathological models, the scenario is not fully understood and constitutes a challenging question. In inflammatory conditions as endotoxemia, increased NO production is mainly due to iNOS induction [21]. Our laboratory has previously shown that the increase in NO steady-state concentration in the heart of endotoxemic animals goes from 22 to 28 nM [4]. It is worth noting that in pathological models, increased levels of NO may exert multiple inhibitory actions on mitochondrial function [6]. This observation can be extended to tissues with higher O2

demand and oxidative metabolism, showing that the NO effect on mitochondrial biogenesis is a general phenomenon.

According to the endosymbiotic theory, mitochondria originated from aerobic free-living bacteria-like organisms (alpha-proteobacteria). At some point in evolution, they were engulfed by primitive, nucleated anaerobic cells to form symbiotic, eukaryotic cells [11]. The organizational features supporting endosymbiotic theory are the presence of a double membrane and its own mtDNA. The mtDNA is a small, circular, double-stranded molecule only 16.5 kb in length. The 37 genes of the human mitochondrial genome encode 13 essential components of the OXPHOS system (i.e., complex I, complex III, complex IV, and FOF1), 22 transfer RNA, and 2 ribosomal RNA [21].

Nevertheless, nuclear genes code for the majority of mitochondrial proteins subsequently translocated into mitochondrion from cytosolic ribosomes. The mtDNA is almost exclusively inherited from the maternal line. A high random mutation rate of mtDNA can be due to the lack of protective histones, inefficient DNA repair mechanisms, and mutagenic effects of mitochondria-generated ROS [22].

Consequently, a large number of single-nucleotide polymorphisms of mtDNA have accumulated among maternal lineages and have diverged as human populations dispersed more widely to different geographical regions of the world. These specific single-nucleotide polymorphisms are known as mtDNA haplogroups [23]. Nine haplogroups have been successively described (H, J, T, U, K, V, W, I, and X), the majority of the European population belonging to haplogroup H (44%) [24].

A longitudinal clinical and genetic study of 150 patients with septic shock revealed that haplogroup H patients presented proportionally better survival than other haplogroups at 28 days, upon hospital discharge and at a six-month follow-up [25]. Furthermore, the Spanish sepsis group of researchers reported a protective effect of haplogroup H on sepsis incidence in a study of 240 patients with postoperative sepsis [26]. Haplogroup H is the most recent addition to the group of European mtDNA but, perhaps paradoxically, is the most common: indeed, increased survival after septic shock may provide one explanation for this. The hypothesis of a direct, functional consequence of improved mitochondrial efficiency arising from this clinical report was subsequently tested by other [27].

Using a transmitochondrial cytoplasmic hybrid cell, they found no difference in mitochondrial bioenergetic capacities or coupling efficiencies when comparing mitochondria from haplogroup H with those from haplogroup T. Haplogroup H survival protection remains poorly understood, and haplogroup effects on mitochondrial proliferation or signaling processes have not yet been fully explored. Other research groups have described the potential consequences of belonging to other haplogroups: for example, haplogroup JT was associated with increased survival in a prospective cohort of 96 patients with severe sepsis and an increased complex IV activity in patients from this haplogroup relative to others [28].

Together, these data indicate a potential effect of genetic haplogroup variants on survival in sepsis cases. The association with functional mitochondrial activity remains unclear; however, no data yet exist on the consequences for cardiac mitochondria during sepsis.

Conclusion

Sepsis-induced cardiomyopathy is a commonly recognised manifestation of sepsis and is associated with worse patient outcomes. There is significant experimental evidence that mitochondrial dysfunction is involved in the development of SIC, although causality has not been definitively established. Data regarding cardiac mitochondrial dysfunction in human sepsis are limited and indirect. Evidence in laboratory studies can be conflicting, likely due to inconsistencies introduced by the models and techniques used. This study will provide insights into mitochondrial biology, the relevance to sepsis, and therapeutic opportunities that possibly emerge.

Competing interests

The authors declare that they have no competing interests.

References

1. Muller-Decker K, Manegold G, Butz H, et al. Inhibition of cell proliferation by bacterial lipopolysaccharides in TLR4-positive epithelial cells: independence of nitric oxide and cytokine release. J Invest Dermatol. 2005;124:553–561. [PubMed]
2. Tobias PS, Soldau K, Gegner JA, Mintz D, Ulevitch RJ. Lipopolysaccharide binding protein-mediated complexation of lipopolysaccharide with soluble CD14. J Biol Chem. 1995; 270:10482–10488. [PubMed]
3. Hood DA, Takahashi M, Connor MK., Freyssenet D. Assembly of the cellular powerhouse: current issues in muscle mitochondrial biogenesis. Exercise and Sport Sciences Reviews 2000; 28(2): 68–73, 2000. View at Scopus
4. Abraham WT, Gilbert EM, Lowes BD, et al. Coordinate changes in Myosin heavy chain isoform gene expression are selectively associated with alterations in dilated cardiomyopathy phenotype. Molecular Medicine Cambridge, Mass. 2002; 8:750–760. [PubMed]
5. Molkentin JD, Kalvakolanu DV, Markham BE. Transcription factor GATA-4 regulates cardiac muscle-specific expression of the alpha-myosin heavy-chain gene. Mol. Cell. Biol 1994;14: 4947–4957. [PubMed]
6. Piantadosi CA, Suliman HB. Mitochondrial transcription factor A induction by redox activation of nuclear respiratory factor 1. J. Biol. Chem 2006; 281: 24–333. [PubMed]
7. Laurie K. Russella, Brian N. Fincka, Daniel P. Kelly. Mouse models of mitochondrial dysfunction and heart failure. Journal of Molecular and Cellular Cardiology 2005; 38(1): 81-91. View at Publisher
8. Crouser ED. Mitochondrial dysfunction in septic shock and multiple organ dysfunction syndrome. Mitochondrion. 2004; 4: 729–741. [PubMed]
9. Huttemann M, Lee I, Samavati L, Yu H, Doan JW: Regulation of mitochondrial oxidative phosphorylation through cell signaling. Biochim Biophys Acta 2007; 1773:1701-1720. [PubMed]
10. Zapelini PH, Rezin GT, Cardoso MR, Ritter C, Klamt F, Moreira JC, et al.: Antioxidant treatment reverses mitochondrial dysfunction in a sepsis animal model. Mitochondrion 2008; 8: 211-218. [PubMed]
11. Yousif NG. Fibronectin promotes migration and invasion of ovarian cancer cells through up-regulation of FAK–PI3K/Akt pathway. Cell biology international 2014; 38 (1): 5-91. [PubMed]

Research Article

12. Hanada T, Yoshimura A. Regulation of cytokine signaling and inflammation. Cytokine Growth Factor Rev 2002; 13: 413-421. [PubMed]

13. Orrenius S, Gogvadze A, Zhivotovsky B: Mitochondrial oxidative stress: implications for cell death. Annu Rev Pharmacol Toxicol 2007; 47:143-183. [PubMed]

14. Echtay KS, Murphy MP, Smith RA.J. Talbot DA, Brand MD. Superoxide activates mitochondrial uncoupling protein 2 from the matrix side. J. Biol. Chem 2002; 77: 47129–47135. Abstract/FREE Full Text

15. Lin TK, Liou CW. Chen SD. et al., Mitochondrial dysfunction and biogenesis in the pathogenesis of Parkinson's disease. Chang Gung Medical Journal 2009; 32(6); 589–599. View at Scopus

16. Hock MB, Kralli A. Transcriptional control of mitochondrial biogenesis and function. Annual Review of Physiology 2009; 71: 177–203. View at Publisher · View at Google Scholar · View at Scopus

17. Lagouge M, Argmann C, Gerhart-Hines Z. et al., Resveratrol improves mitochondrial function and protects against metabolic disease by activating SIRT1 and PGC-1α. Cell 2006; 127(6): 1109–1122. View at Publisher · View at Google Scholar · View at Scopus

18. Suliman HB, Carraway MS, Ali AS, Reynolds CM, Welty-Wolf KE, Piantadosi CA. The CO/HO system reverses inhibition of mitochondrial biogenesis and prevents murine doxorubicin cardiomyopathy. Journal of Clinical Investigation 2007; 117(12): 3730–3741. View at Publisher

19. Nakai A, Yamaguchi O, Takeda T, et al. The role of autophagy in cardiomyocytes in the basal state and in response to hemodynamic stress. Nat Med 2007; 13: 619–624. CrossRefMedline

20. Levine B, Klionsky DJ. Development by self-digestion: molecular mechanisms and biological functions of autophagy. Dev Cell 2004; 6: 463–477. CrossRefMedline

21. Shimomura H, Terasaki F, Hayashi T, Kitaura Y, Isomura T, Suma H. Autophagic degeneration as a possible mechanism of myocardial cell death in dilated cardiomyopathy. Jpn Circ J. 2001; 65: 965–968. CrossRefMedline

22. Valentim L, Laurence KM, Townsend PA, et al. Urocortin inhibits Beclin1-mediated autophagic cell death in cardiac myocytes exposed to ischaemia/reperfusion injury. J Mol Cell Cardiol 2006; 40: 846–852.CrossRefMedline

23. Austin EW, Yousif NG, Ao L, Cleveland JC, Fullerton DA, Meng X. Ghrelin reduces myocardial injury following global ischemia and reperfusion via suppression of myocardial inflammatory response. AJBM 2013; 1(2): 38-48. View at Publisher

24. Klionsky DJ, Abeliovich H, Agostinis P, et al. Guidelines for the use and interpretation of assays for monitoring autophagy in higher eukaryotes. Autophagy 2008; 4: 151–175. Medline

25. Brocheriou V, Hagege AA, Oubenaissa A, Cardiac functional improvement by a human Bcl-2 transgene in a mouse model of ischemia/reperfusion injury. J Gene Med 2000; 2: 326–333. CrossRefMedline

26. Munusamy S, MacMillan-Crow LA. Mitochondrial superoxide plays a crucial role in the development of mitochondrial dysfunctionduring high glucose exposure in rat renal proximal tubular cells Free Radic. Biol. Med 2009; 46:1149–1157 Article View Record in Scopus

27. Ventura-Clapier R, Garnier A, Veksler V. Transcriptional control of mitochondrial biogenesis: the central role of PGC-1alpha Cardiovasc. Res 2008; 79: 208–217 | Full Text via CrossRef

28. Yousif NG, Al-amran FG. Novel Toll-like receptor-4 deficiency attenuates trastuzumab (Herceptin) induced cardiac injury in mice. BMC cardiovascular disorders 2011;11(1): 62. [PubMed]